Adsorption Equilibrium of Water Vapor on Mesoporous Materials

Jae Son Oh,[†] Wang Geun Shim,[†] Jae Wook Lee,*[,‡] Jong Ho Kim,[†] Hee Moon,[†] and Gon Seo*[,†]

Faculty of Applied Chemistry, Chonnam National University, Gwangju 500-757, Korea and Department of Environmental and Chemical Engineering, Seonam University, Namwon 590-711, Korea

Adsorption of water vapor on mesoporous materials such as MCM-41, MCM-48, KIT-1, SBA-1, and SBA-15, which have different pore sizes and shapes, was investigated by using a gravimetric system. In addition, adsorption of water vapor on KIT-1 mesoporous material was examined at 293.15 to 353.15 K. A hybrid isotherm model composed of a Henry isotherm and a Sips isotherm was applied to the analysis of water adsorption on mesopores including its surface adsorption and capillary condensation. The proposed isotherm nicely simulated measured adsorption data over the whole range at these experimental conditions. The capillary condensation of water vapor on mesoporous materials was highly dependent on temperature and pore sizes rather than on their pore shapes.

Introduction

Since the mesoporous materials named as the M41S family were synthesized by Mobil researchers, mesoporous materials with mesopores of 2.0 to 10 nm diameters have been attracting much attention as adsorbents and catalysts.[1] Since then, various mesoporous materials such as MCM-41, MCM-48, MCM-50, KIT-1, SBA-1, and SBA-15 with different pore sizes and shapes were synthesized. MCM-41 and SBA-15 have a hexagonal array of unidirectional pores, while MCM-48 and SBA-1 have a highly ordered bicontinuous cubic pore system. KIT-1 has a disordered three-dimensional network with wormlike channels. The large internal surface area and uniformity of pore size of mesoporous materials increase their application feasibility for separation and removal operations.

Many works on adsorption isotherms of nitrogen on mesoporous materials were reported relating to their pore size and shape. In addition, their adsorption properties of organic vapors suggest their applicability for removal of volatile organic compounds as adsorbents.[2−4] Introduction of aluminum atoms on their skeleton enhances their acidic strength, resulting in strong adsorption of polar materials.

Mesoporous materials, regardless of the structure, type, and composition, usually have plenty of silanol groups on the mesopores because of their amorphous surface structure. A large amount of water can be adsorbed on them because their mesopores are suitable for capillary condensation. A limited study on the adsorption of water vapor, however, has been conducted.[5] Furthermore, the adsorption isotherm model covering the whole range of water adsorption from surface adsorption to capillary condensation has not even been suggested.

The aim of this work, therefore, is to examine the adsorption equilibrium of water vapor on five mesoporous materials: MCM-41, MCM-48, KIT-1, SBA-1, and SBA-15. The adsorption isotherms of water obtained on these mesoporous materials were analyzed using a hybrid isotherm combining the Henry isotherm at low pressure and the Sips isotherm at moderate pressure responsible for capillary condensation.

* To whom correspondence should be addressed. E-mail: jwlee@tiger.seonam.ac.kr. Fax: +82-63-620-0211.
[†] Chonnam National University.
[‡] Seonam University.

Experimental Section

Materials. Five mesoporous materials with different pore sizes and shapes (Table 1) were chosen as adsorbents for adsorption of water vapor. These materials, including MCM-41, MCM-48, KIT-1, SBA-1, and SBA-15, were synthesized according to the procedures described in the literature.[6−12] Hexadecyltrimethylammonium bromide was used as a template for the synthesis of MCM-41, MCM-48, and KIT-1, whereas hexadecyltriethyleneammonium bromide and Pluronic P123 triblock copolymer ($EO_{20}PO_{70}EO_{20}$) were used for SBA-1 and SBA-15, respectively. A Teflon bottle containing the solution mixture of the template and a colloidal silica was preheated in a water bath, and the reaction mixture was stirred. The resultant gel was loaded into an autoclave, and the mixture was hydrothermally treated. The mixture was then filtered and washed with deionized water. After drying at 333 K for overnight, the dried solid was then calcined in air at 873 K for 10 h.

Apparatus and Procedure. X-ray diffraction (XRD) patterns of synthesized mesoporous materials were recorded on an X-ray diffractometer (Rigaku D/MAX-III) using a Cu Kα X-ray and Ni filter at 35 kV and 15 mA. The XRD pattern of SBA-15 mesoporous material was recorded from $\theta = 0.7°$ for observing its large mesopores. Nitrogen adsorption and desorption isotherms were measured at 77 K using a Micromeritics ASAP 2010 automatic analyzer. Before the measurements, the samples were outgassed for 2 h in the degas port of the adsorption apparatus. The measurement of the adsorption−desorption isotherms required 1 day. Their BET surface areas were determined from the adsorption isotherms of nitrogen. In addition, their pore size distributions were also calculated from the adsorption branches of the isotherms by using the Barrett, Joyner, and Halenda (BJH) method.

The adsorption amount of water vapor was measured by a quartz spring balance, which was placed in a closed glass system. An adsorbent sample of 0.1 g was placed on a quartz basket attached to the end of a quartz spring. Prior to the exposure to water vapor, adsorbent samples were evacuated to 1×10^{-3} Pa for 10 h at 573.15 K. The high

10.1021/je0301390 CCC: $25.00
Published on Web 08/02/2003

Table 1. Physical Properties of Mesoporous Materials

property	MCM-41	MCM-48	KIT-1	SBA-1	SBA-15
pore structure	hexagonal	cubic	disorderd 3-D	cubic	hexagonal
surface area/$m^2 \cdot g^{-1}$	981	983	923	940	645
mean pore size/Å	30	28	29	21	50

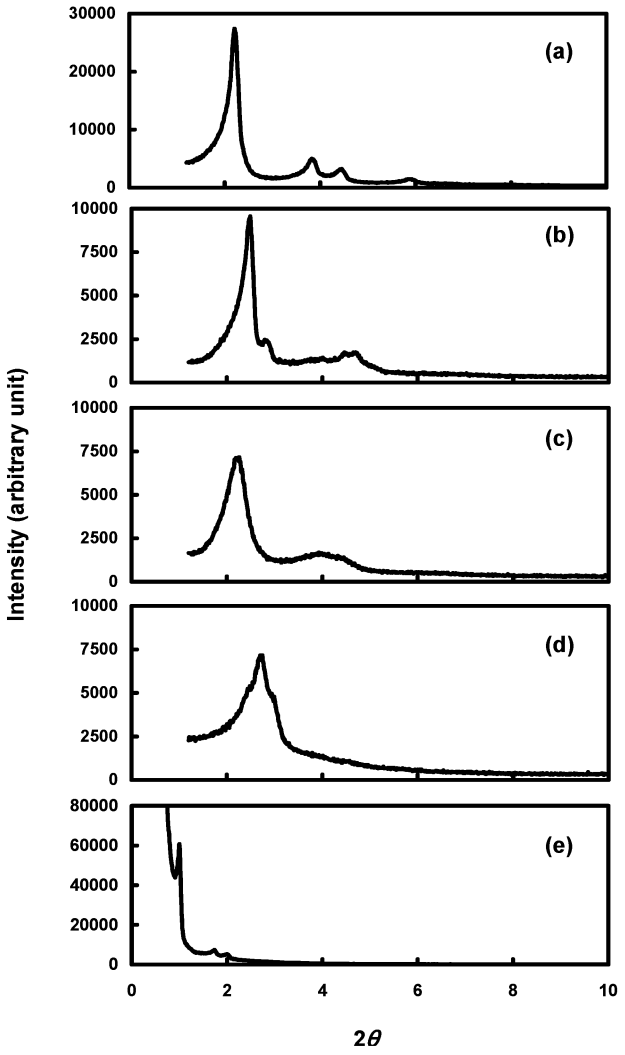

Figure 1. XRD patterns of mesoporous materials: a, MCM-41; b, MCM-48; c, KIT-1; d, SBA-1; e, SBA-15.

vacuum system was composed of a turbomolecular pump (Osaka type TH50) and a rotary vacuum pump (Kaauga BSE215). Pirani and Penning vacuum gauges (Edwards Series 1000) were used for the measurement of the vacuum. The pressure of the water vapor was measured using a Baratron absolute pressure transducer (MKS Instrument type 127) with the accuracy ±0.15%. Water vapor was generated in a small tubular reservoir that was maintained at a constant temperature. During the adsorption experiment, the adsorption cell was placed in a water bath with temperature controlled to within ±0.05 K. The increase in mass of the adsorbent samples with water adsorption was measured by using a digital displacement meter (MKS type PDR-C-1C). The measurement of the adsorption−desorption isotherms required 3 days for water vapor.

Results and Discussion

Figure 1 shows the XRD patterns of mesoporous materials. The XRD patterns of all materials are very well-defined

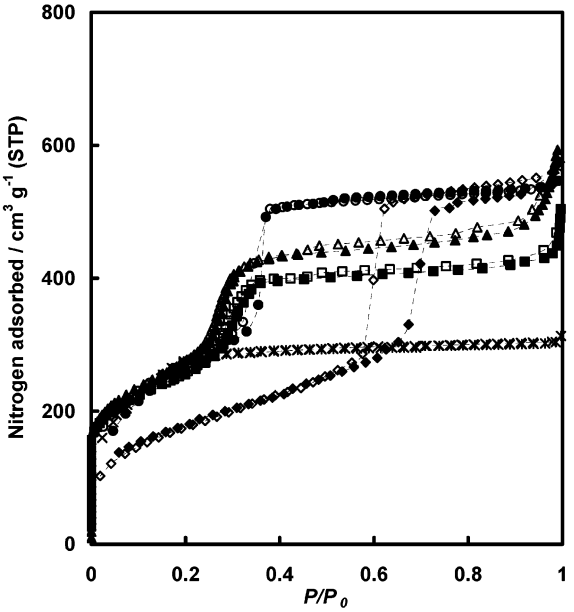

Figure 2. Nitrogen adsorption (closed symbols) and desorption (open symbols) isotherms on mesoporous materials at 77 K: ○, MCM-41; △, MCM-48; □, KIT-1; ∗, SBA-1; ◇, SBA-15.

and characteristic of well-ordered hexagonal, cubic, or disordered 3-dimensional materials which are in good agreement with those previously reported.[1−3,9,11,12] Mesoporous materials usually show sharp increases in their adsorption isotherms of nitrogen because of capillary condensation. The pressure responsible for capillary condensation is related to the sizes of the mesopores, and the increase in the adsorption amount by capillary condensation corresponds to the volumes of mesopores. Five mesoporous materials used in this study show different adsorption isotherms of nitrogen in terms of shapes, the pressure responsible for capillary condensation, and pore volume, as shown in Figure 2. The MCM-41, MCM-48, KIT-1, and SBA-15 show typical nitrogen adsorption isotherms of mesoporous materials with capillary condensation in mesopores. On the contrary, the SBA-1 shows a type I isotherm in the IUPAC classification, suggesting that it has very small mesopores causing capillary condensation at extremely low pressure. Capillary condensation in mesopores of the MCM-41 type is observed at around $P/P_0 = 0.35$, while that of MCM-48 and KIT-1 is observed at around $P/P_0 = 0.30$. The similar pressures for the capillary condensations of the MCM-41, MCM-48, and KIT-1 suggest a similarity in pore size due to the use of the same template. The high pressure for the capillary condensation of the SBA-15 at around $P/P_0 = 0.70$ indicates that it has considerably large mesopores compared to the cases of other mesoporous materials. Also, the pore size shows an important effect on the presence or absence of hysteresis.

Figure 3 shows the pore size distributions of the five mesoporous materials obtained from their nitrogen desorption isotherms using the BJH method. They have a very narrow monodisperse pore size distribution. The determined average pore diameters of the MCM-41, MCM-48, and KIT-1, which were synthesized using the same template, were around 30 Å. Those of the SBA-1 and SBA-15,

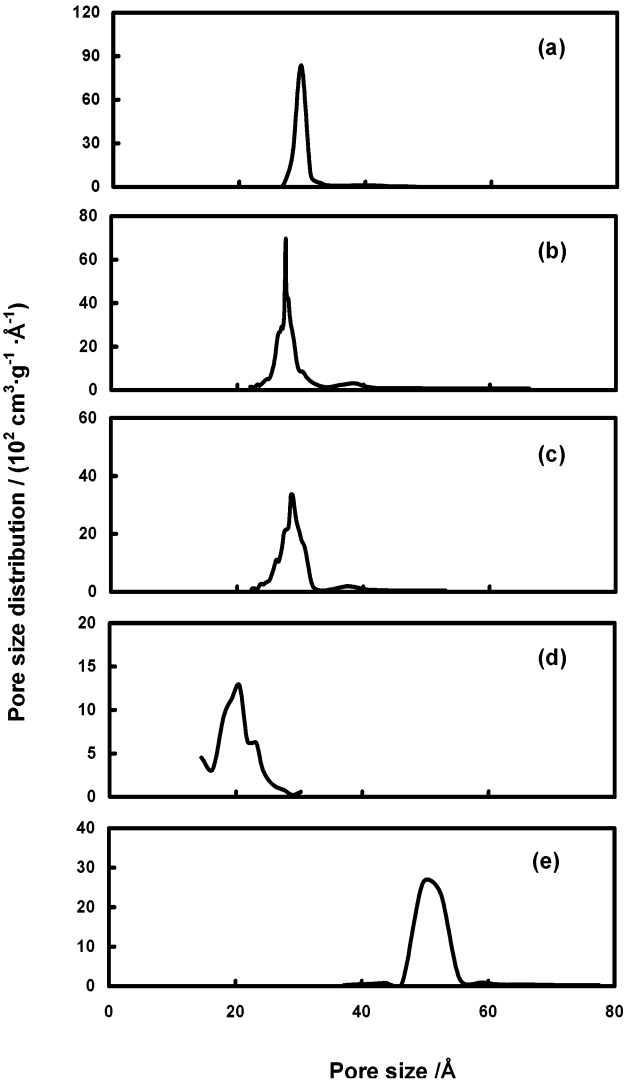

Figure 3. Pore size distribution of mesoporous materials: a, MCM-41; b, MCM-48; c, KIT-1; d, SBA-1; e, SBA-15.

however, were as different as 21 and 50 Å, respectively, because they were synthesized using different synthetic reagents and at different conditions.

Figure 4 illustrates the adsorption isotherms of water vapor on the five mesoporous materials. Although they have different pore sizes and shapes, the obtained isotherms are similar. The adsorption amount of water linearly increases at low pressure, while capillary condensation occurs at moderate pressure. These isotherms can be identified as the unusual type V on the basis of IUPAC classification, which represents the mesoporous materials having a hydrophobic surface.[5,13]

The pressures responsible for capillary condensation of water were different according to mesoporous materials: $P/P_0 = 0.45$ for the SBA-1, $P/P_0 = 0.55$ for the KIT-1, $P/P_0 = 0.65$ for both the MCM-41 and the MCM-48, and $P/P_0 = 0.80$ for the SBA-15. The overlapping potential of the walls more readily overcomes the translational energy of adsorptive molecules in a mesopore so that condensation occurs at a lower pressure in a mesopore than that normally required on an open surface. Thus, as the relative pressure is increased, condensation occurs first in pores of smaller size and progresses into the larger pores. The smallest pores of the SBA-1 among the five mesoporous materials cause the lowest pressure of water for its capillary condensation. We also observed the capillary condensation of

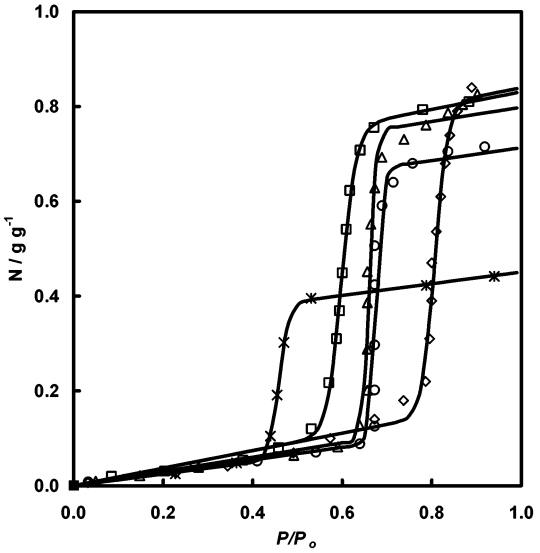

Figure 4. Adsorption isotherms of water vapor on mesoporous materials at 293.15 K: ○, MCM-41; △, MCM-48; □, KIT-1; ∗, SBA-1; ◇, SBA-15; —, simulated Henry−Sips isotherm.

Table 2. Adsorption Isotherm Data of Water Vapor on Mesoporous Materials at 293.15 K

MCM-41		MCM-48		KIT-1	
P/P_0	N/g·g^{-1}	P/P_0	N/g·g^{-1}	P/P_0	N/g·g^{-1}
0.033	0.008	0.049	0.009	0.085	0.020
0.221	0.031	0.148	0.021	0.203	0.031
0.410	0.052	0.279	0.039	0.271	0.040
0.541	0.070	0.492	0.064	0.378	0.054
0.639	0.088	0.590	0.082	0.458	0.080
0.672	0.125	0.639	0.127	0.531	0.120
0.673	0.202	0.656	0.201	0.570	0.217
0.674	0.297	0.657	0.288	0.587	0.310
0.675	0.424	0.658	0.386	0.594	0.369
0.676	0.506	0.659	0.451	0.600	0.449
0.689	0.591	0.664	0.552	0.609	0.541
0.714	0.640	0.672	0.628	0.617	0.623
0.757	0.680	0.689	0.693	0.640	0.708
0.836	0.705	0.738	0.731	0.671	0.756
0.918	0.715	0.787	0.761	0.780	0.793
		0.836	0.787	0.883	0.810
		0.869	0.804		
		0.902	0.826		

SBA-1		SBA-15			
P/P_0	N/g·g^{-1}	P/P_0	N/g·g^{-1}	P/P_0	N/g·g^{-1}
0.227	0.025	0.032	0.007	0.800	0.390
0.364	0.048	0.229	0.027	0.805	0.470
0.439	0.105	0.344	0.041	0.810	0.536
0.455	0.191	0.491	0.069	0.820	0.610
0.470	0.302	0.573	0.100	0.830	0.680
0.530	0.395	0.672	0.140	0.840	0.739
0.788	0.422	0.737	0.180	0.857	0.790
0.939	0.442	0.786	0.220	0.889	0.840
		0.795	0.310		

water on the SBA-15 at a higher pressure than that on the MCM-41 and MCM-48 because of its large pores. The difference in the pressure responsible for the capillary condensation of water on the KIT-1 and MCM-41, however, indicates that the shape of mesopores also affects the capillary condensation, even though its effect is not significant. The adsorption isotherm data of water vapor at 293.15 K on the five mesoporous materials are presented in Table 2.

On the other hand, adsorption of water on mesoporous materials is significantly dependent on temperature. Figure 5 shows the adsorption isotherms of water vapor on the

Table 3. Adsorption Isotherm Data of Water Vapor on KIT-1 in Terms of Temperatures

293.15 K		298.15 K		303.15 K		308.15 K		313.15 K		323.15 K		353.15 K	
P/kPa	*N*/g·g^{-1}	*P*/kPa	*N*/g·g^{-1}	*P*/kPa	*N*/g·g^{-1}	*P*/kPa	*N*/g·g^{-1}	*P*/kPa	*N*/g·g^{-1}	*P*/kPa	*N*/g·g^{-1}	*P*/kPa	*N*/g·g^{-1}
0.198	0.020	0.299	0.027	0.550	0.037	0.550	0.034	0.372	0.031	0.743	0.029	0.277	0.006
0.476	0.031	0.897	0.057	0.826	0.057	1.046	0.078	0.877	0.058	1.266	0.046	0.515	0.008
0.634	0.040	1.305	0.106	1.211	0.091	1.431	0.108	1.249	0.077	1.844	0.063	0.912	0.012
0.884	0.054	1.414	0.169	1.541	0.160	1.651	0.120	1.488	0.090	2.009	0.067	1.269	0.013
1.070	0.080	1.469	0.225	1.623	0.243	1.844	0.139	1.754	0.104	2.146	0.071	1.586	0.018
1.242	0.120	1.506	0.297	1.656	0.315	1.981	0.162	1.940	0.116	2.256	0.076	1.823	0.021
1.333	0.217	1.532	0.388	1.689	0.400	2.036	0.185	2.126	0.130			1.982	0.023
1.374	0.310	1.550	0.462	1.714	0.484	2.091	0.215	2.312	0.144			2.141	0.027
1.389	0.369	1.574	0.574	1.740	0.569	2.119	0.267					2.299	0.029
1.403	0.449	1.632	0.658	1.816	0.648	2.131	0.314						
1.424	0.541	1.741	0.698	2.009	0.685	2.142	0.375						
1.443	0.623	2.075	0.730	2.201	0.698	2.147	0.440						
1.497	0.708					2.163	0.517						
1.569	0.756					2.205	0.595						
1.823	0.793					2.280	0.624						
2.065	0.810												

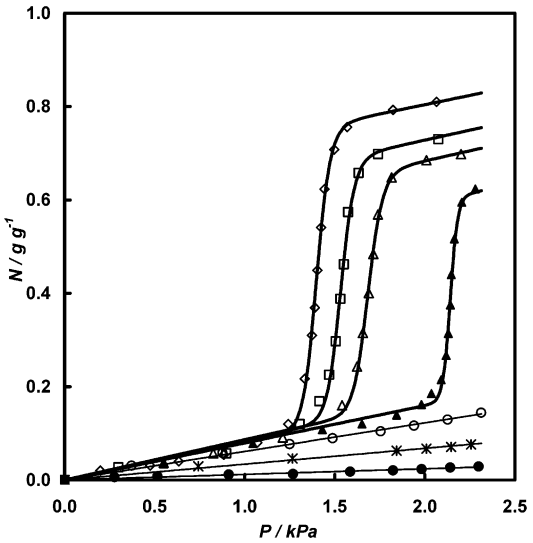

Figure 5. Adsorption isotherms of water vapor on KIT-1 in terms of temperatures: ◇, 293.15 K; □, 298.15 K; △, 303.15 K; ▲, 308.15 K; ○, 313.15 K; ∗, 323.15 K; ●, 353.15 K; —, simulated Henry isotherm; —, simulated Henry−Sips isotherm.

KIT-1 at various temperatures. The linear increases in the adsorption amount of water are the same on all the isotherms at low pressure, but the adsorption behavior of water differs with adsorption temperature. Under our experimental conditions below 2.5 kPa, capillary condensation occurs up to 308.15 K. A large difference in the adsorption amount of water with a small change in temperature from 308.15 K and 313.15 K suggests that mesoporous material can be used as an effective dehumidifier to remove a large amount of water per mass in an adsorption−desorption dehumidifying cycle. Table 3 lists the isotherm data of water vapor on the KIT-1 at seven different temperatures.

Adsorption isotherms play a key role both in designing water removal processes in chemical plants and in modeling adsorption−desorption dehumidifiers.[14,15] One simple adsorption model, however, is not adequate to describe water adsorption in mesopores because water adsorbs with forming both the adsorbed layer on the inner surface and the capillary condensation. Surface adsorption is dominant at low pressure while condensed water fills mesopores at high pressure. Hybrid adsorption models, therefore, are required to simulate adsorption behavior of water on mesopores over the whole pressure range.

Among the many isotherms tested for the simulation of water, we found that the hybrid isotherm model of the Henry and the Sips isotherms with four parameters nicely fitted the experimental adsorption data. The proposed isotherm model is as follows:

$$N = K(P/P_0) + \frac{mb(P/P_0)^n}{1 + b(P/P_0)^n} \quad (1)$$

where N is the adsorption amount, P is the pressure of water, P_0 is the saturation pressure of water at the adsorption temperature, K is the Henry isotherm parameter, and m, b, and n are the Sips isotherm parameters.[16] Four parameters (K, m, b, n) of the hybrid isotherm were determined by a nonlinear least-squares fitting routine of Nelder−Mead simplex method. The Henry isotherm parameter for surface adsorption has a physical meaning in the thermodynamic view, whereas the Sips isotherm parameters describe only the capillary condensation of water at moderate pressure. It is evident that b and n—relating to adsorption strength—are very sensitive for the capillary condensation. However, the interpretation of their variance with adsorption temperature and species was not tried because the intrinsic physical meanings of the Sips parameters were not clearly understood.

The solid lines (Figures 3 and 4) are the simulated results using the determined parameters of the hybrid isotherms listed in Tables 4−6. Also, the goodness-of-fit was calculated by comparing the square of residuals (SOR), defined as follows:

$$\mathrm{SOR} = \frac{1}{2}\sum(N_{\mathrm{exp}} - N_{\mathrm{cal}})^2 \quad (2)$$

Table 4. Parameters of the Hybrid Henry−Sips Isotherm for Water Vapor on Mesoporous Materials at 293.15 K

	MCM-41	MCM-48	KIT-1	SBA-1	SBA-15
K	1.23×10^{-1}	1.51×10^{-1}	1.85×10^{-1}	1.23×10^{-1}	1.85×10^{-1}
m	5.78×10^{-1}	6.48×10^{-1}	6.46×10^{-1}	3.27×10^{-1}	6.55×10^{-1}
b	2.64×10^{15}	5.15×10^{16}	2.34×10^{8}	9.84×10^{13}	2.21×10^{5}
n	90.5	92.6	37.5	41.3	57.3
SOR	3.26×10^{-2}	2.19×10^{-2}	1.02×10^{-3}	3.10×10^{-5}	6.67×10^{-3}

Table 5. Parameters of the Hybrid Henry−Sips Isotherm for Water Vapor on KIT-1 at 293.15, 298.15, 303.15, and 308.15 K

	293.15 K	298.15 K	303.15 K	308.15 K
K	7.93×10^{-1}	8.53×10^{-2}	8.48×10^{-2}	7.97×10^{-2}
m	6.45×10^{-1}	5.58×10^{-1}	5.14×10^{-1}	4.35×10^{-1}
b	3.23×10^{-6}	2.92×10^{-8}	3.10×10^{-10}	1.14×10^{-35}
n	37.6	40.6	42.0	106.0
SOR	1.02×10^{-3}	1.37×10^{-3}	6.81×10^{-4}	1.67×10^{-3}

Table 6. Parameters of the Henry Isotherm for Water Vapor on KIT-1 at 313.15, 323.15, and 353.15 K

	313.15 K	323.15 K	353.15 K
K	6.12×10^{-2}	3.39×10^{-2}	1.21×10^{-2}
SOR	5.38×10^{-5}	1.59×10^{-5}	1.15×10^{-5}

As defined in eq 2, the SOR is an absolute value and the magnitude is dependent on the goodness-of-fit as well as the number of experimental points.[17] Simulated isotherms using the hybrid isotherm model are highly coincidental with the equilibrium adsorption data. Thus, we expect that the hybrid isotherm proposed in this study will be widely applicable for kinetic and dynamic studies on the adsorption and desorption of water vapor on mesoporous materials composed of both surface adsorption and capillary condensation.

Conclusion

Adsorption equilibria of water vapor on the five mesoporous materials MCM-41, MCM-48, KIT-1, SBA-1, and SBA-15 were classified as the unusual type V, representing surface adsorption and capillary condensation on their mesopores. The size of the mesopores and temperature highly affected the pressure responsible for capillary condensation, while the effect of pore shape is relatively small. The proposed hybrid isotherm model which combines the Henry and the Sips isotherms describes well the adsorption data including surface adsorption and capillary condensation of water vapor even with a set of four parameters, suggesting that the hybrid isotherm model will be useful for the simulation of adsorption behavior of water vapor on mesoporous materials.

Note Added after ASAP Posting. This article was released ASAP on 8/2/2003. To clarify the data presented in Figure 5, the adsorption isotherm of water vapor on KIT-1 in terms of temperature from P/P_0 to P has now been presented employing the capillary condensation corresponding to each temperature instead of the reference vapor pressure (293.15 K) as in the original posting. The text under Figure 5 and the data in Tables 3, 5, and 6 also have been changed for the same reason. In addition, the units in Table 2 have been corrected. The paper was reposted on 9/10/2003.

Literature Cited

(1) Beck, J. S.; Vartuli, J. C.; Roth, W. J.; Leonowicz, M. E.; Kresge, C. T.; Schmitt, K. D.; Chu, C. T.-W.; Olson, D. H.; Sheppard, E. W.; McCullen, S. B.; Higgins, J. B.; Schlenker, J. L. A New Family of Mesoporous Molecular Sieves Prepared with Liquid Crystal Templates. *J. Am. Chem. Soc.* **1992**, *114*, 10834−10843.

(2) Hartmann, M.; Bischof, C. Mechanical Stability of Mesoporous Molecular Sieve MCM-48 Studied by Adsorption of Benzene, *n*-Heptane, and Cyclohexane. *J. Phys. Chem. B* **1999**, *103*, 6230−6235.

(3) Zhao, X. S.; Lu, G. Q. Organophilicity of MCM-41 Adsorbents Studied by Adsorption and Temperature-Programmed Desorption. *Colloids Surf., A* **2001**, *179*, 261−269.

(4) Paulis, M.; Gandia, L. M.; Gil, A.; Sambeth, J.; Odriozola, J. A.; Montes, M. Influence of the Surface Adsorption−Desorption Processes on the Ignition Curves of Volatile Organic Compounds (VOCs) Complete Oxidation over Supported Catalysts. *Appl. Catal. B* **2000**, *26*, 37−46.

(5) Inagaki, S.; Fukushima, Y. Adsorption of Water Vapor and Hydrophobicity of Ordered Mesoporous Silica, FSM-16. *Microporous Mesoporous Mater.* **1998**, *21*, 667−672.

(6) Jung, K. H.; Chung, K. H.; Kim, M. Y.; Kim, J. H.; Seo, G. IR Study of the Secondary Reaction of Ethylene Oxide over Silver Catalyst Supported on Mesoporous Material. *Korean J. Chem. Eng.* **1999**, *16*, 396−400.

(7) Ryoo, R.; Joo, S. H.; Kim, J. M. Energetically Favored Formation of MCM-48 from Cationic-Neutral Surfactant Mixtures. *J. Phys. Chem. B* **1999**, *103*, 7435−7440.

(8) Lee, J. W.; Lee, J. W.; Shim, W. G.; Suh, S. H.; Moon, H. Adsorption of Chlorinated Volatile Organic Compounds on MCM-48. *J. Chem. Eng. Data* **2003**, *48*, 381−387.

(9) Kim, W. G.; Kim, M. W.; Kim. J. H.; Seo, G. Dispersion Measurement of Heteropoly Acid Supported on KIT-1 Mesoporous Material. *Microporous Mesoporous Mater.* **2003**, *57*, 113−120.

(10) Park, S. S.; Choe, S. J.; Park, D. H. The Effect of Phosphate Treatment on Nickel Dispersion on MCM-41 Mesoporous Material. *Korean J. Chem. Eng.* **2003**, *20*, 256−261.

(11) Kruk, M.; Jaroniec, M.; Ryoo, R.; Kim, J. M. Characterization of High-Quality MCM-48 and SBA-1 Mesoporous Silicas. *Chem. Mater.* **1999**, *11*, 2568−2572.

(12) Kruk, M.; Jaroniec, M.; Ko, C. H.; Ryoo, R. Characterization of the Porous Structure of SBA-15. *Chem. Mater.* **2000**, *12*, 1961−1968.

(13) Rouquerol, F.; Rouquerol, J.; Sing, K. *Adsorption by Powders and Porous Solids*; Academic Press: London, 1999.

(14) Ruthven, D. M. *Principles of Adsorption and Adsorption Processes*; John Wiley & Sons: New York, 1984.

(15) Yang, R. T. *Gas Separation by Adsorption Processes*; Butterworths: Boston, 1987.

(16) Sips, R. Structure of a Catalyst Surface. *J. Chem. Phys.* **1948**, *16*, 490−495.

(17) Malek, A.; Farooq, S. Comparison of Isotherm Models for Hydrocarbon Adsorption on Activated Carbon. *AIChE J.* **1996**, *42*, 3191−3201.

Received for review February 24, 2003. Accepted June 13, 2003. The authors appreciate the financial support of KOSEF (Grant Number 2001-130700-002-3 to G.S. and Grant Number R-01-2001-000-00414-0 (2002) to J.W.L. and H.M.).

JE0301390